STUDY OF PROPERTIES AND PERFOMANCE OF CEMENTED CARBIDE TOOLS COATED WITH $Al_{1-x}Cr_xN$ (LOW ALUMINUM)

Renato Françoso de Ávila, renato.avila@jfsudestemg.edu.br
Jalon de Morais Vieira, jalon.vieira@ifsudestemg.edu.br
Sara Del Vecchio, sara.vecchio@ifsudestemg.edu.br
Instituto Federal de Educação, Ciência e Tecnologia – IF Sudeste MG, Campus Juiz de Fora, Núcleo de Mecânica, Brazil

Rafael Drumond Mancosu, rafael.mancosu@indt.org.br
Instituto Nokia de Tecnologia – IndT, Manaus-AM, Brazil

Alisson Rocha Machado, alissonm@mecanica.ufu.br
Universidade Federal de Uberlândia, FEMEC/LEPU, Uberlândia - MG, Brazil

Leonardo Roberto da Silva, lrsilva@deii.cefetmg.br
Centro Federal de Educação Tecnológica de Minas Gerais - CEFET-MG, DEMEC, Belo Horizonte, Brazil

Abstract. *The performance of coated tools is of fundamental importance in machining processes. Nowadays some research has been carried out to investigate the influence of nano structured coatings (different stoichiometric ratios of chemical elements), particularly the influence of aluminum content in Ti-Al-N and Cr-Al-N ternary ceramic coatings, on the machinability of several ferrous materials. The main purpose of the present work is to study the properties and to investigate the machining performance of K10 straight grade of cemented carbide inserts coated with $Al_{1-x}Cr_xN$, low aluminum content ($x \leq 0.3$). The tools, after coated by electron beam evaporation plasma-assisted PVD (EBPAPVD) technique, had the chemical compositions, thickness and structure (EDS and XRD analysis) of their coatings determined. These tools were then tested in turning of grey cast iron under real cutting conditions. Uncoated (WC-Co 6%) and comercial Ti-Al-N coated tools were also tested for comparisons. Preliminary results indicated the best performance of the $Al_{1-x}Cr_xN$ with low aluminum content.*

Keywords: *$Al_{1-x}Cr_xN$ low aluminum, characterization techniques, continuous cutting.*

1. INTRODUCTION

Ti-Al-N and Cr-Al-N ternary coatings processed by EBPAPVD (electron beam evaporation plasma-assisted PVD) either as mono or multilayer have become extremely important to several and strategic industrial applications such as automotive and aeronautic industries. These coatings are thermodynamically metastable and possess high micro hardness value, high oxidation stability, low thermal conductive and relatively low coefficient of friction against steel and several materials for different applications in the metal-mechanical industries. Because of these remarkable advantages, these coatings have been investigated mainly for metal cutting operations (turning, milling and drilling) since the 90´s, providing high metal removal rates (Avila, *et al.*, 2008, Paldey *et al.*, 2003; Hultman, 2000 and Karlsson *et al.*, 2000).

Research shows that Ti-Al-N and Cr-Al-N ternary coatings have different crystalline structures (single phase crystalline cubic structure, mixed phases - cubic and hexagonal structures and hexagonal structure only) according to the Al (% at.) contents (Mayrhofer, *et al.*, 2008, Reiter *et al.*, 2005 and Zhou, *et al.*, 1999).

Properties of coatings, in general, are strongly dependent on the film structure. This fact is particularly important when the Al concentration (x) is increased in some ranges. Ti_{1-x} Al_x N films present a cubic B1 structure, which is the same structure as in Ti-N films, when Al concentration (x) is less than 0,6 (Zhou *et al.*, 1999). When the Al concentration varies from 0.6 to 0.7, two phases are present: a cubic B1 structure (NaCl model) corresponding to a substitution solid solution of (Ti,Al)N and a hexagonal B4 structure (ZnS-Wurtzite model) corresponding to an Al-N phase. Under these conditions the hardness and the Young modulus decrease rapidly. Therefore the functional properties of a coating, like thermal conductivity, oxidation and wear resistance, depend on the coating's structural properties.

This paper investigates the cutting performance of $Al_{1-x}Cr_xN$ - low aluminum content (controlled deposition stoichiometric ratios of constituents) in turning of gray cast iron under real cutting conditions. For comparative analysis uncoated (WC-Co 6%) and Ti_{1-x} Al_x N ternary coatings (commercial deposition stoichiometric ratios of constituents) were also tested.

2. EXPERIMENTAL PROCEDURE

2.1. Coating process and characterization

K10 ISO grade of cemented carbide (WC-Co 6%) inserts with ISO geometry SNMA 120408 (without chip breaker) were used as substrates. Prior to the deposition of the hard film, a thin layer (100 – 300nm) of Ti was applied to the substrate in order to ensure satisfactory adhesion.

Ternary coatings of Ti_{1-x} Al_x N and $Al_{1-x}Cr_xN$ low aluminum content were processed by electron beam evaporation plasma-assisted PVD (EBPAPVD) like commercial and controlled deposition stoichiometric ratios of constituents, respectively. For the $Al_{1-x}Cr_xN$ coating the levels of aluminum present was predetermined as $x \leq 0.3$ (low aluminum). This aluminum content was defined taking into account the results of previous work (Ávila, *et al.,* 2010), that has considered: pure Al, time of evaporation, temperature of deposition, among other parameters of the deposition chamber. The chemical composition of the Ti_{1-x} Al_x N and $Al_{1-x}Cr_xN$ thin films was analyzed by SEM photomicrographs on metallographic cross-sections. The value of thickness encountered was less than 5.0 μm for both coatings.

X-ray diffractometry (XRD) using a Phillips PW1710 diffractometer was performed to identify phases which had been formed during the coating process. The radiation used was Cu-k_α (λ = 0,154056nm) and the diffractograms were recorded by scanning the samples at a 2θ step of 0.02° per second from 10 to 110°.

2.2 Machining Tests

Bars of gray cast iron (chemical composition: 3.44 % C, 2.38 % Si, 0.005%S, 0.16 % Mn, 0.038 % S, 0.05 % P and 0.03 % Mg; 0.16%Mn with pearlite in a ferrite matrix and average hardness of 144HB) with 85.0 mm of diameter and 250 mm long were used as workpieces. The cemented carbide inserts were mounted on a tool holder, ISO code PSDNN2525-M12, resulting in the following geometry: approach angle, χ_r = 45°, included angle ε_r = 95°, cutting edge inclination angle λ_s = -5°, rake angle γ_o=-6° and clearance angle α_o = 6°.

The machining trials were carried out in a CNC lathe (Romi - 30D) with maximum spindle speed of 4000rpm and power of 7.5kW. The cutting conditions were established after preliminary machining trials. Table 1 presents the cutting parameters used and Fig 1 shows a detail of a test.

Table 1. Cutting parameters

Tribological System	v_c (m/min)	f (mm/rev)	a_p (mm)
Substrate WC-Co (6%)	200	0.20	2.0
Ti_{1-x} Al_x N / WC-Co (6%)			
$Al_{1-x}Cr_xN$ / WC-Co (6%)			

The tests were conducted without cutting fluid and two replicas for each condition were performed. A new cutting edge was used in each test.

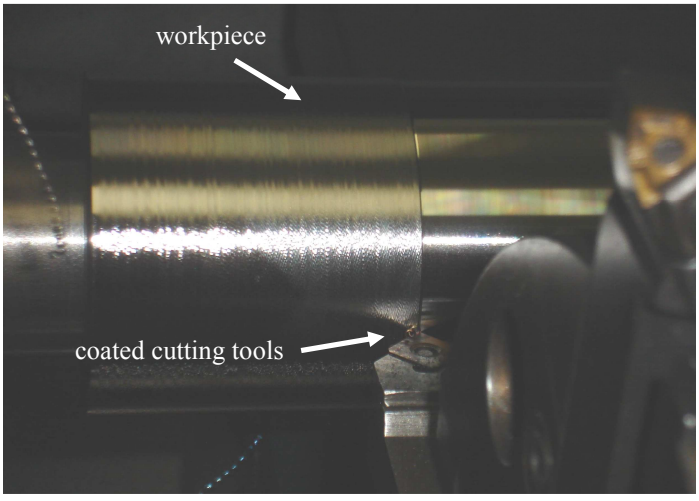

Figure 1. Details of a test: workpiece and coated cutting tools

3 RESULTS AND DISCUSSION

3.1. Chemical compositions

Figure 2 shows the qualitative results obtained by EDS (*Energy Dispersive Spectroscopy*) analysis on areas of each nanostructured ternary coatings. Calculated values of aluminum content are showed in Tab. 2.

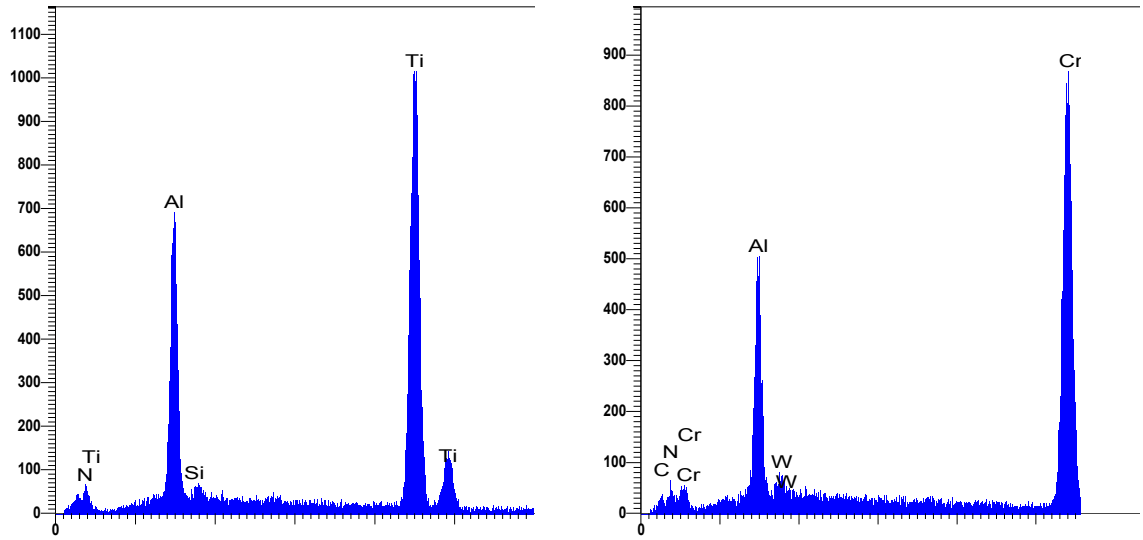

(a) (b)

Figure 2. EDS analysis: (a) Ti_{1-x} Al_x N (commercial deposition) and (b) $Al_{1-x}Cr_xN$ (low aluminum)

Tabela 2. Average of Aluminum contents on nanostructured ternary coatings

	Aluminum (at.)
$Al_{1-x}Cr_xN$ (low aluminum) (controlled deposition stoichiometric ratios of Al)	~21.7
Ti_{1-x} Al_x N (commercial deposition stoichiometric ratios of Al)	~56.0

3.2. Cross-section of the inserts

SEM photomicrographs on metallographic cross-sections of the inserts are shown Fig. 3.

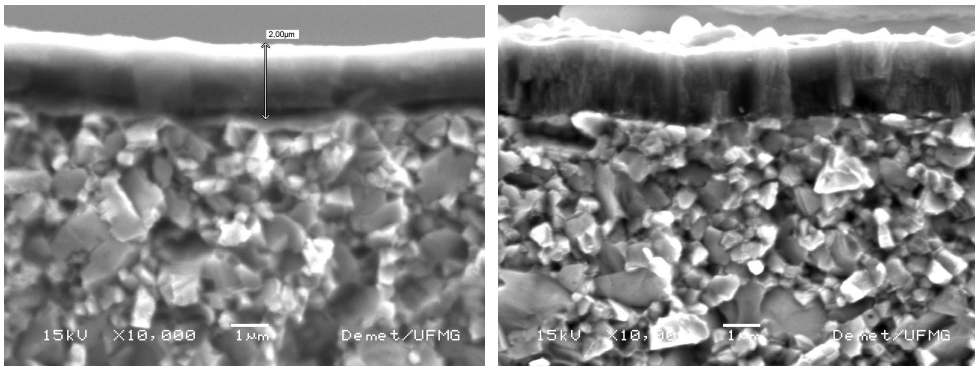

(a) (b)

Figure 3. SEM micrographs: (a) $Al_{1-x}Cr_xN$ / WC-Co (6%) (6%) and (b) Ti_{1-x} Al_x N / WC-Co (6%)

All films are very dense and ostensibly not columnar. Similar qualitative results were showed by Reiter *et al.* (2005). The film thicknesses were in the range of 2.0 to 3.0 μm. These values are very important when considering the probabilities of internal residual stress increase and delamination occurrences.

3.3. XRD analysis

X-ray diffractograms of the uncoated and coated cutting tools are shown in Fig. 4. Table 3 shows the main phases observed.

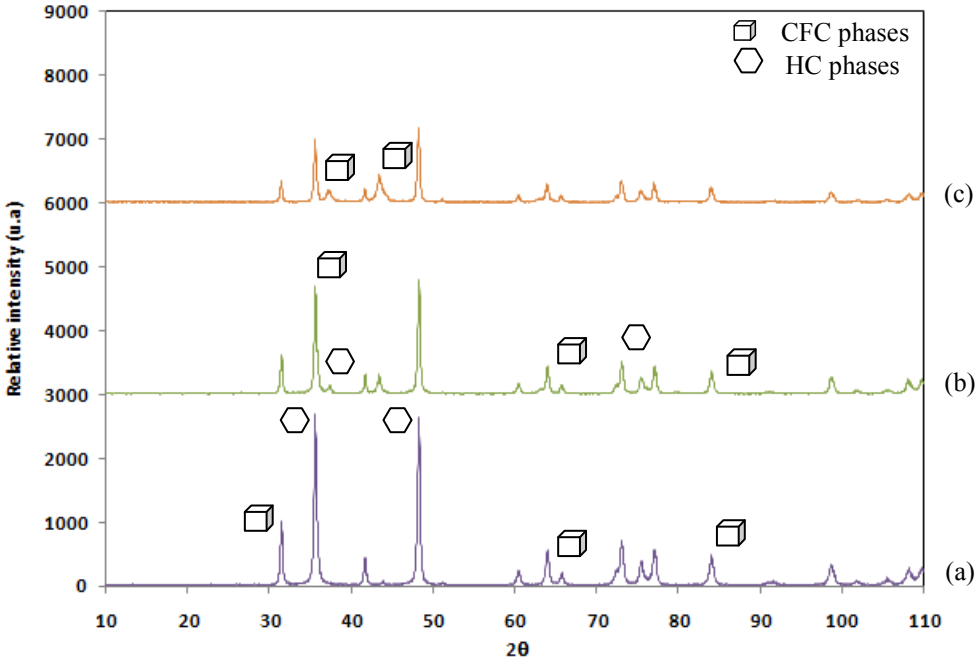

Figure 4. X-ray diffractograms: (a) Uncoated WC-Co (6%), (b) Ti_{1-x} Al_x N / WC-Co (6%) and (c) $Al_{1-x}Cr_xN$ / WC-Co (6%) tools

Table 3. XRD – Main phases and crystallographic orientation

Tribological systems	Main phases and crystallographic orientation
Substrate WC-Co (6%)	• (200) TiC(cfc) • (0001) WC(hc) • (1011) WC(hc) • (111) Co(cfc) • (311) Co(cfc)
Ti_{1-x} Al_x N / WC-Co (6%)	• (200) Ti_{1-x} Al_x N (cfc) • (0002) AlN (hc) • (220) Ti_{1-x} Al_x N (cfc) • (1013) AlN (hc) • (311) Ti_{1-x} Al_x N (cfc)
$Al_{1-x}Cr_xN$ / WC-Co (6%)	• (111) $Al_{1-x}Cr_xN$ (cfc) • (200) $Al_{1-x}Cr_xN$ (cfc)

XRD results show the effects of hexagonal phases of the WC-Co (6%) substrate on both coatings in study. This effect is bigger in the Ti_{1-x} Al_x N / WC-Co (6%) tribological systems than in the $Al_{1-x}Cr_xN$ / WC-Co (6%). The main crystalline phases present were WC (hc), TiC (cfc) and Co (cfc) for the WC-Co (6%) substrate. These crystalline phases were also identified in similar tool materials (He, *et al.*, 2002 and Zambrano *et al*, 1998).

A mixed phase [Ti_{1-x} Al_x N (cfc) and AlN (hc)] was identified in the Ti_{1-x} Al_x N film and only a single phase [$Al_{1-x}Cr_xN$ (cfc)] in the $Al_{1-x}Cr_xN$ film.

Avila *et al.* (2008) showed X-ray diffraction results, obtained from the as-deposited (Ti,Al)N system. Two phases were observed, the cubic B1- NaCl similar phase, corresponding to a substitution solid solution of (Ti,Al)N and a hexagonal B4 structure corresponding to an Al-N phase with Al concentration (x) estimated in 0.56. In that study

serious problems of adhesion and poor machining performance of Ti-Al-N coatings on cemented carbide substrates were related after characterizations techniques and turning tests of AISI 4340 steel.

Hasegawa *et al.* (2005) show X-ray diffraction for $Al_{1-x}Cr_xN$ films with chromium concentration (x) ranging from 0 to 1.0. The NaCl like structures for x equal to 0.6 was observed. When Al content was increased the hexagonal B4 structure (ZnS-Wurtzite model) was identified.

The influence of substrate´s phases and the formation of mixed phases for some ranges for Al concentration (x) in both ternary coatings on adhesion properties and cutting performance are inevitable but require further investigation for clarifications.

3.4. Machining tests

Figure 5 shows preliminary results obtained from the machining tests.

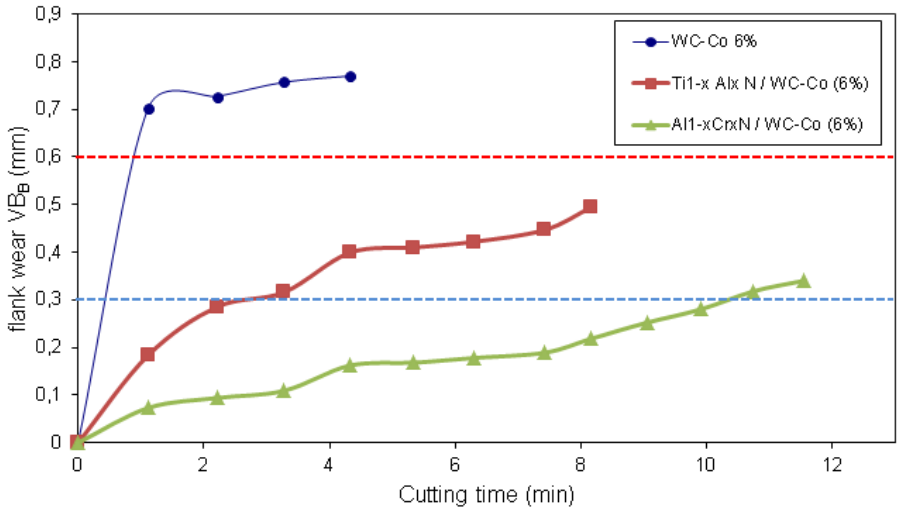

Figure 5. Flank wear evolution (VB_B) with average cutting time for uncoated and coated cutting tools (cutting speed = 200m/min, feed rate = 0.20mm/rev and depth of cutting = 2.0mm)

Considering the flank wear VB_B parameters established in ISO 3685/1993 standard the best performance was obtained for $Al_{1-x}Cr_xN$ / WC-Co (6%). The next best result is showed by the Ti_{1-x} Al_x N (commercial deposition stoichiometric ratios of Al) coated tools and the uncoated WC-Co (6%) presented the worse results.

The poorer performance of Ti_{1-x} Al_x N (commercial deposition stoichiometric ratios of Al) than the $Al_{1-x}Cr_xN$ coatings can be associated to their mixed phases (cfc - NaCl model B1) and (hc - ZnS model B4). According to Zhou *et al*. (1999), when the Al concentration increases and the phase transition from B1 to B4 structure occurs, the compressive residual stress decreases sharply and tensile stresses are generated. Besides the adverse structure and mechanical properties relative to the wear, the machining conditions employed during the turning trials (high sliding speed, work material with high hardness) probably led to severe wear of the cutting tool. Similar occurrence was reported in the turning of AISI 4340 with worst performance to Ti-Al-N coatings when compared to uncoated tools (Avila *et al.,* 2008).

However, it is strongly advised that further investigations should be conducted if clarification and control of the stoichiometric system of the coating films is envisaged. These include nano-hardness measurements, tests under other cutting conditions, machining force components monitoring, among other options.

Figure 6 shows the scanning electron micrographs of the rake and clearance faces of $Al_{1-x}Cr_xN$ / WC-Co (6%) coated carbide tool after this tests. A maximum flank wear on the flank face was identified in this ternary coating for all replicas. The tool of Figure 6 also shows a huge spalling on its rake face.

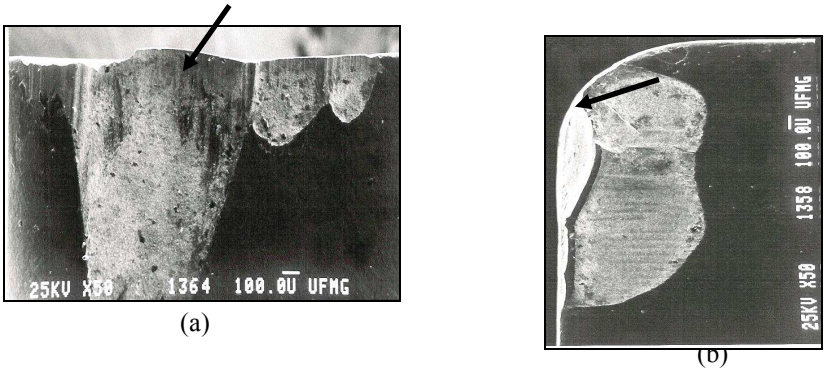

(a) (b)

Figure 6. Tool wear after turning gray cast iron with $Al_{1-x}Cr_xN$ / WC-Co (6%) coated tools at v_c = 200 m/min, f = 0.20 mm/rev and a_p = 2.0 mm; (a) clearance face and (b) rake face

4. CONCLUSIONS

The results suggest that the Ti_{1-x} Al_x N film used in the present investigation do not show good performances during turning of gray cast iron, although it exhibit good high temperature stability, as reported in the literature. The performance of Ti_{1-x} Al_x N films strongly depends on its microstructure that presented double phases. On the other hand, in the $Al_{1-x}Cr_xN$ films (low Al content) only the cubic phase was identified. This fact suggests isotropic conditions, less values of residual stress and consequently best performance in real cutting conditions. This have been proved in the machining tests.

5. ACKNOWLEDGEMENTS

Authors would like to thank CNPq, CAPES and FAPEMIG (Brazil) for financial support.

6. REFERENCES

Ávila, R. F., Godoy C., Abrão, A. M. and Lima, M. M., 2008, "Topographic analysis of the crater wear on TiN, Ti(C,N) and (Ti,Al)N coated carbide tools", Wear, Vol. 265, pp. 49-56.

Ávila, R. F., Vieira, J. M., Mancosu, R. D., Machado, A. R., Silva, R. B., 2010, "Influence of nanostructured coatings on surface finish of AISI 1047 steel", 18th IFHTSE Congress – International Federation for Heat Treatment and Surface Engineering, July 26-30, CD Proceedings, , Rio de Janeiro, Brazil, 2010, pp. 5175 – 5186.

Hasegawa, H., Kawate, M. and Tetsuya, S., 2005, "Effects of Al Contents on Microstructures of $Cr_{1-x}Al_xN$ and $Zr_{1-x}Al_xN$ Films Synthesized by Cathodic Arc Method. Surface and Coatings Technology, Vol. 200, pp. 2409 – 2413.

Hultman, L., 2000, "Thermal stability of nitride thin films", Vaccum, Vol. 57, pp. 1 – 30.

Karlsson, L., Hultman, L., Johansson, M. P., Sundgren, J-E. and Ljungcrantz, H., 2000, "Growth, microstructure and mechanical properties of arc evaporeted TiC_xN_{1-x} ($0 \leq x \leq 1$) films", Surface and Coatings Technology, Vol. 126, pp. 1 – 14.

Mayrhofer, P. H., Willmann, H. and Reiter, A. E., 2008, "Structure and phase evolution of Cr-Al-N coatings during anneling, Surface and Coantings Technology, Vol. 202, pp. 4935-4938.

Paldey, S. and Deevi, S. C., 2003, "Single layer and multilayer wear resistant coatings of (Ti, Al)N: a review", Materials Science and Engineering A, Vol. 342, pp. 58 – 79.

Reiter, A. E., Derflinger, V. H., Hanselmann, B., Bachmann, T. and Sartory, B. 2005, "Investigation of the properties of Al1-xCrxN coatings prepared by cathodic arc evaporation", Surface & Coatings Technology, Vol. 200, pp. 2114 – 2122.

Zhou. M., Makino. Y., Nose. M. and Nogi. K, 1999. "Phase transition and properties of Ti-Al-N thin films prepared by rf-assisted magnetron sputtering", Thin Solid Films, Vol. 339, pp. 203 – 208.

6. RESPONSIBILITY NOTICE

Authors are the only responsible for the printed material included in this paper.